Optical Materials: X 17 (2023) 100213

Contents lists available at ScienceDirect

Optical Materials: X

journal homepage: www.elsevier.com/locate/omx

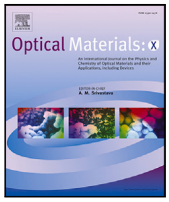

Microscopic understanding of lithium defect on lanthanide luminescence in $NaYF_4$ lattices from first principles

Xian Qin *, Xiaogang Liu *

Department of Chemistry, National University of Singapore, 3 Science Drive 3, Singapore 117543, Singapore

ARTICLE INFO

Keywords:
Lithium doping
Lanthanide luminescence
Isovalent substitution
Interstitial defect
DFT
Lithium–oxygen cluster

ABSTRACT

Lithium doping has been widely employed to modulate the photoluminescence of lanthanide-doped crystals. Despite its effectiveness, the underlying mechanism remains debatable. Using cubic sodium yttrium fluoride as a model crystal, first-principles calculations indicate that neutral substitution of host sodium with lithium ions can occur, irrespective of synthesis conditions. Unlike lithium substitution, the formation of lithium interstitials is likely accompanied by the substitution of F^- with O^{2-} ions. The lithium substitution shows negligible influence on the electronic structures of the host crystal and the 4f orbital energies of lanthanide ions. By comparison, the lithium-oxygen defect pairs could induce self-absorption losses in lanthanide luminescence or produce ligand-to-metal charge transfer states that could populate lanthanide 4f states.

1. Introduction

Lanthanide photoluminescence originating from intra-4f transitions has been witnessed in a wide range of applications, including three-dimensional display, data encryption, microlasing, and high-energy photodetection, as well as imaging-guided therapeutics [1–3]. Despite the great success, the luminescence intensity of given lanthanide-activated phosphors remains low, mainly due to the parity-forbidden nature of the intra-band transition [4]. To this end, considerable effort has been made to enhance lanthanide luminescence, such as core–shell passivation, isovalent/anisovalent co-doping, dye sensitization, and plasmonic coupling [5–7].

Lithium incorporation has widely proven effective in enhancing lanthanide luminescence. However, the underlying mechanism remains elusive. For instance, lithium-induced enhancement has been ascribed to distortion of spectroscopic site symmetries, improvement of crystallinity, suppression of quenching centers, or shrinkage of lattice constants [8–10]. Notably, it has been reported that successful incorporation of lithium ions largely depends on synthetic approaches [11]. Specifically, Li^+ ions were detected in lanthanide-doped Y_2O_3 microparticles prepared by solid-state reactions, while the particles prepared by wet chemistry approaches involving centrifugation and washing steps were free of Li^+ dopants. In this regard, identifying the presence and distribution of lithium dopants in host lattices is important from both scientific and practical perspectives. However, experimental characterization of lithium incorporation at the atomic level remains challenging, impeding its ensuing mechanistic study of luminescence enhancement.

By virtue of their ability to characterize defects, first-principles calculations have been widely used to predict and identify lattice defects in solids [12,13]. Herein, we investigate the doping of lithium ions in fluoride crystals using first-principles calculations based on the frame of density functional theory (DFT). The cubic sodium yttrium fluoride crystal (α-NaYF4) was chosen for its generalizability to host lanthanide emitters and its structural simplicity. Given the same valence electrons, lithium ions can easily replace sodium ions. In addition, we hypothesize that lithium ions could form interstitial defects owing to their small ionic size and low packing density of the cubic lattice.

2. Results and discussion

We employed a cubic $NaYF_4$ supercell model containing 144 atoms to investigate the thermodynamic stability of lithium incorporation. Lithium substitution (Li_{Na}) and interstitial (I_{Li}) were generated by replacing one Na atom with a Li atom and inserting one Li atom into the interstitial space, respectively (Fig. 1 and Supplementary Fig. S1). The calculated phase diagram indicates that α-$NaYF_4$ can only form in a narrow range of relative chemical potentials. Fluoride-rich (point A), fluoride-medium (point B), and fluoride-poor (point C) conditions were selected to estimate the formation energies of the Li_{Na} and I_{Li} defects.

For lithium substitution, the optimized atomic structure suggests negligible lattice distortion, as manifested by the slight shrinkage in the first coordination environment of Li^+ compared with Na^+ ions (Fig. 2a). In contrast, the incorporation of Li^+ at interstitial sites generates a

* Corresponding authors.
E-mail addresses: chmqinx@nus.edu.sg (X. Qin), chmlx@nus.edu.sg (X. Liu).

https://doi.org/10.1016/j.omx.2022.100213
Received 21 September 2022; Received in revised form 22 October 2022; Accepted 28 October 2022
Available online 24 November 2022

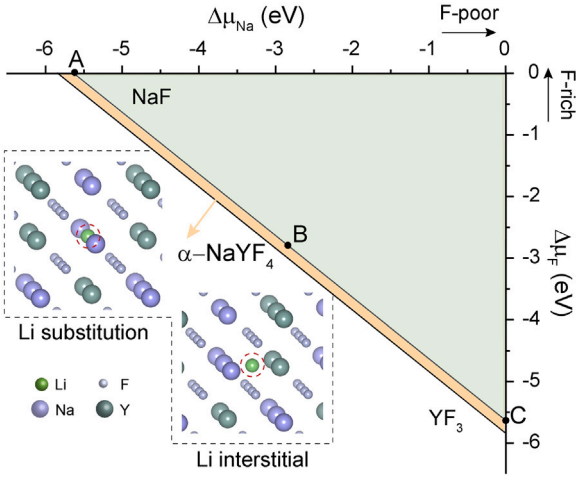

Fig. 1. Atomic illustration of lithium substitution and interstitial defects in a cubic sodium yttrium fluoride lattice and the calculated thermodynamic stability diagram. $\Delta\mu_{Na}$ and $\Delta\mu_F$ are the relative chemical potentials of sodium and fluoride, respectively, relative to their elemental substances. Points A, B, and C denote fluoride-rich, fluoride-medium, and fluoride-poor conditions, respectively.

marked lattice distortion. For example, host fluoride ions underwent considerable rearrangement upon lithium intercalation, even for the distant fluorides (Fig. 2b). By plotting the formation energies as a function of relative chemical potentials and Fermi level (ϵ_F), we found that singly positively charged Li_{Na} defects are not stable over the entire range of ϵ_F and singly negatively charged Li_{Na} defects can form only when ϵ_F is highly close to the host conduction band edge (Fig. 2c). As a result, the neutral Li_{Na} defects dominate, irrespective of the synthetic conditions. Notably, these neutral substitutions are highly likely to form owing to their moderate formation energies of ~0.68 eV. In the case of I_{Li} defects, the formation energy versus the Fermi level suggests that the neutral interstitial is not stable over the whole range of ϵ_F and a singly positively charged interstitial dominates (Fig. 2d). Specifically, this charged interstitial has a higher formation probability when the ϵ_F shifts toward the valence band edges of the host.

We next investigated the effect of these defects on the electronic structures of α-$NaYF_4$. The calculated density of states shows that Li_{Na} does not introduce mid-gap states and the bandgap remains unaltered (Fig. 3a). This suggests that lithium substitution has little impact on the optical properties of the fluoride host. We further studied the electronic interaction between Li and lanthanide dopants. Nd^{3+} and Yb^{3+} were chosen as model ions because their ionic sizes are larger and smaller, respectively, than that of Y^{3+}. From an energetic point of view, lanthanide ions randomly replace Y^{3+} host ions, irrespective of the presence of lithium ions. As a result, lanthanides can be close to lithium ions or far from them. By plotting the density of states of crystals containing Li–Nd or Li–Yb clusters, we found that lithium ions exert a negligible influence on the 4f orbital energies of lanthanides (Fig. 4b and c).

In the case of α-$NaYF_4$:I_{Li} systems, we only considered the singly positively charged lithium interstitial because of its thermodynamic stability. Similarly, such charged defects do not introduce mid-gap states (Supplementary Fig. S2). Considering that crystals are electrically neutral, charged defects are generally compensated by defects with opposite charges. Fluoride interstitials or substitution of F^- with O^{2-} ions (O_F) may be effective in neutralizing the charged lithium interstitials in α-$NaYF_4$ crystals. We excluded the fluoride interstitial-mediated charge compensation because fluoride interstitials are unlikely to form under F-poor or medium conditions [14].

Despite the use of an inert atmosphere during synthesis, the presence of oxygen impurities has been observed in sodium yttrium fluoride phosphors, making them promising for charge compensation [15]. Instead of well separated from each other, I_{Li} and O_F defects tend to form I_{Li}–O_F pairs due to the electrostatic attraction between these oppositely charged defects. The calculated formation energies indicate that I_{Li}–O_F clusters can form under F-medium or F-poor conditions (Fig. 4a). In contrast, it is nearly impossible to replace fluoride with oxygen ions under F-rich conditions (Supplementary Fig. S3). Unlike Li_{Na} defects, single positive and negative I_{Li}–O_F clusters are more stable than their neutral counterpart when ϵ_F shifts toward the valence and conduction band edges of the host, respectively. Notably, the thermodynamic transition level of (0/+) is located at 1.57 eV above the host valence band edge, and the level of (−/0) is at 1.28 eV below the host conduction band edge. These transition levels suggest that the defective host may participate in lanthanide-activated photoluminescence processes. For example, lanthanide emission could induce electronic transitions at these defect sites.

The calculated density of states shows that the presence of I_{Li}–O_F pairs leads to multiple mid-gap states carried by O 2p orbitals (Fig. 4b). Further substitution of Nd^{3+} for Y^{3+} in the first coordination shell of an I_{Li}–O_F pair slightly affects the energies of the Nd 4f orbitals (Fig. 4c). Notably, we found hybridization between Nd 4f and O 2p orbitals, suggesting relaxation of the parity selection rule to some extent. Additionally, it is likely that electronic transitions from O 2p to Nd 4f orbitals occur upon photoexcitation (Fig. 4d and e). This shows

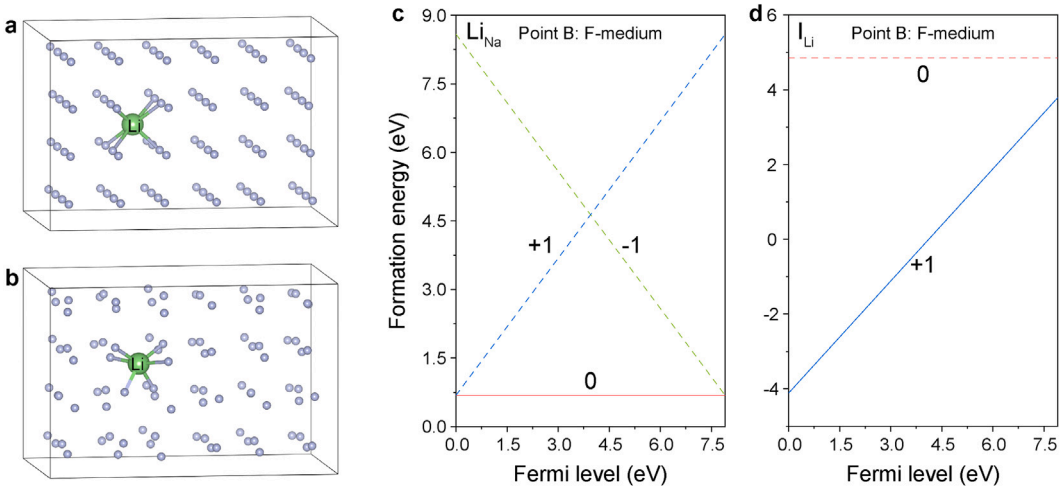

Fig. 2. Optimized atomic structures of α-$NaYF_4$ crystals containing (a) Li_{Na} and (b) I_{Li} lattice defects. (c, d) Calculated formation energies of Li_{Na} and I_{Li} (charged and neutral) as a function of Fermi energy under F-medium conditions. Gray spheres represent fluoride atoms. Note that sodium and yttrium atoms are removed for better visualization.

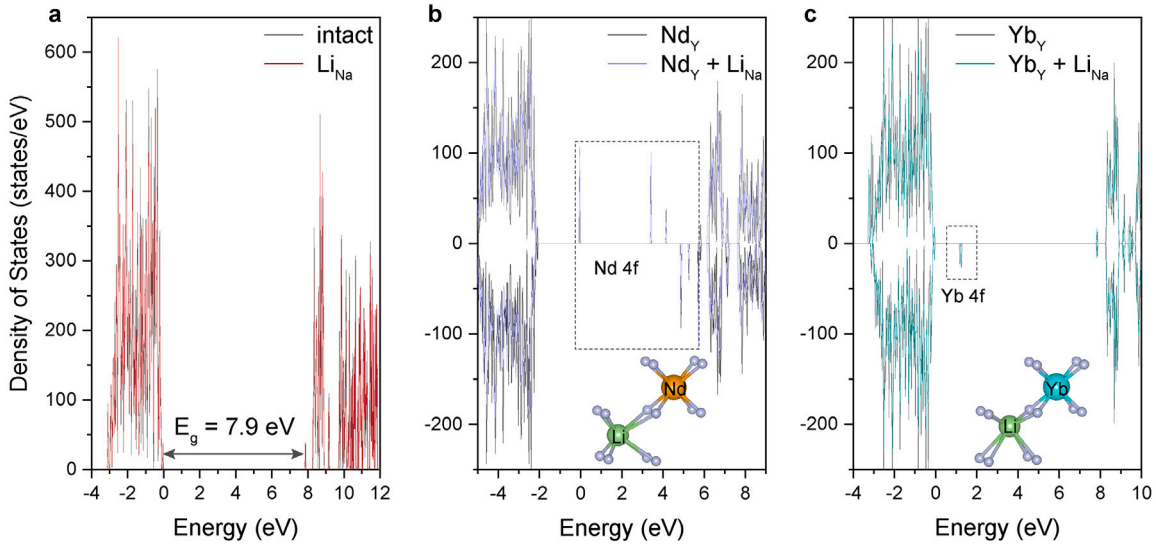

Fig. 3. Calculated total density of states of (a) α-$NaYF_4$ and α-$NaYF_4$:Li, (b) α-$NaYF_4$:Nd and α-$NaYF_4$:Li,Nd, and (c) α-$NaYF_4$:Yb and α-$NaYF_4$:Li,Yb crystals. Insets shown in (b) and (c) are the optimized atomic structures of Li–Nd and Li–Yb clusters, respectively. Gray spheres represent fluoride atoms.

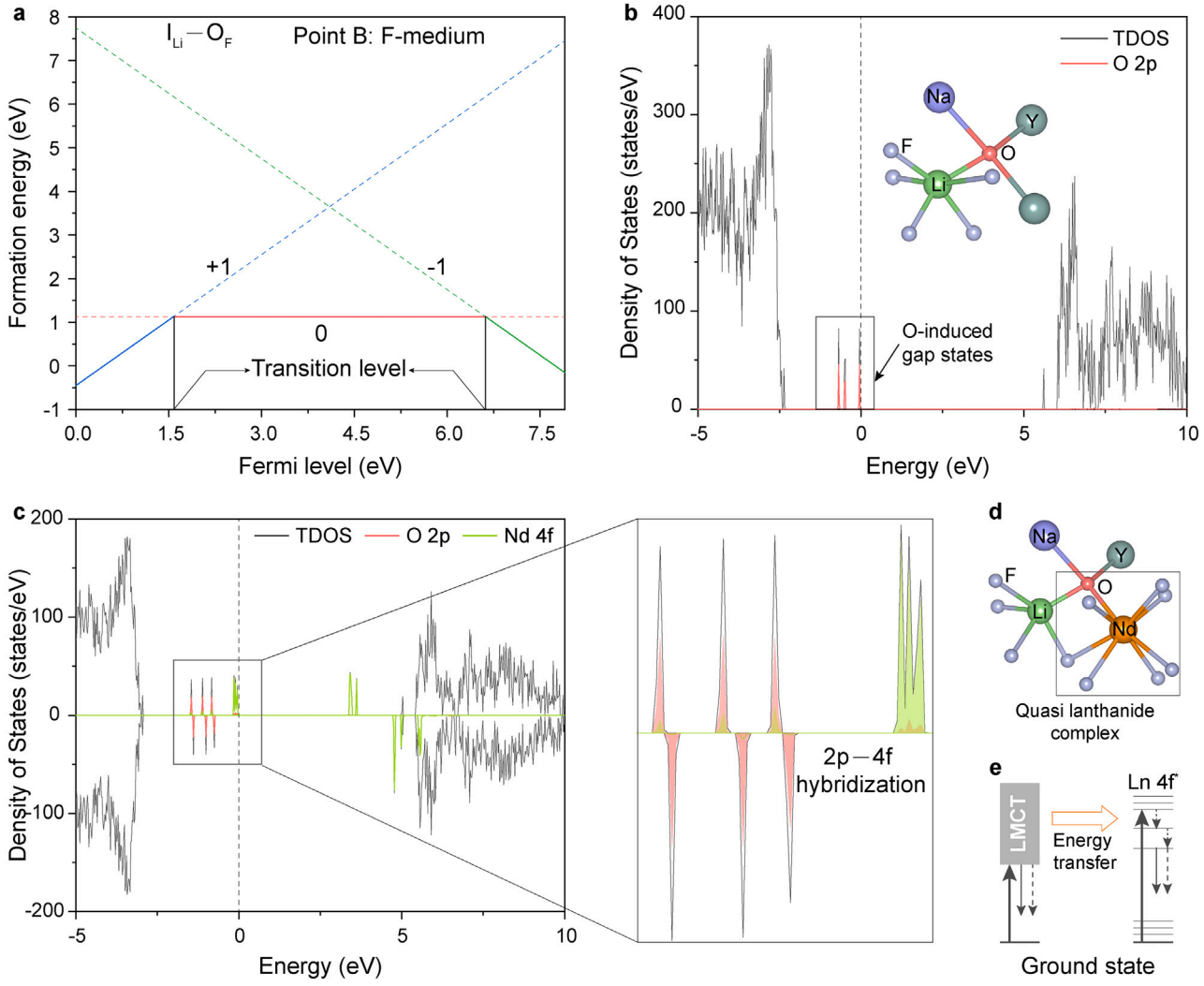

Fig. 4. (a) Calculated formation energies of I_{Li}–O_F defect complex (charged and neutral) as a function of Fermi energy under F-medium conditions. (b, c) Calculated total and projected density of states of α-$NaYF_4$:Li,O and α-$NaYF_4$:Li,O,Nd crystals, respectively. Inset is the optimized atomic structure of an I_{Li}–O_F cluster. (d) Optimized atomic structure of a Li–O–Nd cluster. (e) Schematic energy transfer diagram from ligand-to-metal charge transfer (LMCT) states to lanthanide 4f states. Solid thick, solid thin, and dashed arrows represent absorption, emission, and nonradiative decay, respectively.

a close resemblance to ligand-to-metal charge transfer in lanthanide complexes [16,17]. In the case of Yb^{3+}, we found stronger hybridization between Yb 4f and O 2p orbitals compared with Nd^{3+}, which can be ascribed to the more migratory nature of Yb 4f electrons (Supplementary Fig. S4) [18]. Moreover, a considerable change occurred in the energy gap between the occupied and empty 4f orbitals upon oxygen incorporation. This suggests that I_{Li}–O_F pairs could alter the 4f–4f transition energies of Yb^{3+} ions and Yb-involved energy transfer processes.

3. Conclusion

In conclusion, we have systematically investigated the formation of lithium-associated defects in cubic sodium yttrium fluoride crystals and their influence on the optical properties of lanthanide ions using first-principles calculations. The moderate formation energy suggests that the substitution of host Na^+ by Li^+ can easily occur, even under sodium-rich conditions, mainly due to the close valency similarity between Na^+ and Li^+ ions. Moreover, lithium substitution barely affects the electronic structures of the host lattice and the positions of lanthanide 4f orbitals. Unlike the point defect of Li_{Na}, the calculation shows that the formation of Li interstitials is probably accompanied by the substitution of F^- by O^{2-} ions. The presence of thermodynamic transition levels of I_{Li}–O_F pairs suggests that self-absorption may occur in lanthanide luminescence. Additionally, the ligand-to-metal charge transfer transitions could contribute to lanthanide luminescence through energy transfer. These findings provide atomic insights into the Li-mediated tuning of lanthanide luminescence that could apply to other dopant-activated luminescent materials.

4. Computational methods

The energetic and electronic DFT calculations were performed using the Vienna ab initio simulation package (VASP) with the projector augmented wave method [19,20]. Perdew–Burke–Ernzerhof generalized gradient approximation was employed to describe the exchange–correlation interactions between electrons [21,22]. The screed-exchange hybrid functional HSE06 with 12% Hartree–Fock exchange interaction was employed to calculate the electronic structures of systems under study [23,24]. The energy cutoff of the plane wave basis expansion was set at 520 eV, and the energy and force convergence criteria were set at 1×10^{-6} eV and 0.01 eV/Å, respectively. A gamma-centered k-point sampling of $1 \times 1 \times 2$ was used for the supercell. Methodologies used for the calculation of formation energy and thermodynamic transition level are illustrated in refs [14,25]. For determining the chemical potential of lithium and oxygen elements, O_2 gas, lithium bulk, LiF, and Y_2O_3 were considered as secondary competing phases.

CRediT authorship contribution statement

Xian Qin: Conceptualization, Methodology, Calculation, Writing – original draft. **Xiaogang Liu:** Conceptualization, Supervision, Writing – review & editing, Funding acquisition.

Declaration of competing interest

The authors declare that they have no known competing financial interests or personal relationships that could have appeared to influence the work reported in this paper.

Data availability

Data will be made available on request.

Acknowledgments

This work was supported by National Research Foundation, Singapore, the Prime Minister's Office of Singapore under its NRF Investigatorship Programme (Award No. NRF-NRFI05-2019-0003).

Appendix A. Supplementary data

Supplementary material related to this article can be found online at https://doi.org/10.1016/j.omx.2022.100213.

References

[1] J.-C.G. Bünzli, Lanthanide photonics: shaping the nanoworld, Trends Chem. 1 (8) (2019) 751–762.
[2] X. Chen, T. Sun, F. Wang, Lanthanide-based luminescent materials for waveguide and lasing, Chem. Asian J. 15 (1) (2020) 21–33.
[3] B. Zheng, J. Fan, B. Chen, X. Qin, J. Wang, F. Wang, R. Deng, X. Liu, Rare-earth doping in nanostructured inorganic materials, Chem. Rev. 122 (6) (2022) 5519–5603.
[4] M.P. Hehlen, M.G. Brik, K.W. Krämer, 50Th anniversary of the Judd–Ofelt theory: An experimentalist's view of the formalism and its application, J. Lumin. 136 (2013) 221–239.
[5] S. Wen, J. Zhou, P.J. Schuck, Y.D. Suh, T.W. Schmidt, D. Jin, Future and challenges for hybrid upconversion nanosystems, Nature Photonics 13 (12) (2019) 828–838.
[6] S. Liu, L. Yan, J. Huang, Q. Zhang, B. Zhou, Controlling upconversion in emerging multilayer core–shell nanostructures: from fundamentals to frontier applications, Chem. Soc. Rev. (2022).
[7] A.N.C. Neto, M.A.C. dos Santos, O.L. Malta, R. Reisfeld, Effects of spherical metallic nanoparticle plasmon on 4f-4f luminescence: a theoretical approach, in: Metal Nanostructures for Photonics, Elsevier, 2019, pp. 19–36.
[8] C. Zhao, X. Kong, X. Liu, L. Tu, F. Wu, Y. Zhang, K. Liu, Q. Zeng, H. Zhang, Li^+ ion doping: an approach for improving the crystallinity and upconversion emissions of $NaYF_4$: Yb^{3+}, Tm^{3+} nanoparticles, Nanoscale 5 (17) (2013) 8084–8089.
[9] H. Lin, D. Xu, D. Teng, S. Yang, Y. Zhang, Simultaneous size and luminescence control of $NaYF_4$: Yb^{3+}/RE^{3+} (RE = Tm, Ho) microcrystals via Li^+ doping, Opt. Mater. 45 (2015) 229–234.
[10] T. Pang, W. Lu, W. Shen, Chromaticity modulation of upconversion luminescence in $CaSnO_3$: Yb^{3+}, Er^{3+}, Li^+ phosphors through Yb^{3+} concentration, pumping power and temperature, Physica B 502 (2016) 11–15.
[11] M.L. Debasu, J.C. Riedl, J. Rocha, L.D. Carlos, The role of Li^+ in the upconversion emission enhancement of $(YYbEr)_2O_3$ nanoparticles, Nanoscale 10 (33) (2018) 15799–15808.
[12] A. Alkauskas, M.D. McCluskey, C.G. Van de Walle, Tutorial: Defects in semiconductors—Combining experiment and theory, J. Appl. Phys. 119 (18) (2016) 181101.
[13] J. Cai, C.-G. Ma, M. Yin, Factors influencing the structure of the complex-defects in AF_2:RE^{3+} (A=Ca, Sr and Ba): A first-principles study, J. Lumin. 250 (2022) 119058.
[14] X. Qin, L. Shen, L. Liang, S. Han, Z. Yi, X. Liu, Suppression of defect-induced quenching via chemical potential tuning: a theoretical solution for enhancing lanthanide luminescence, J. Phys. Chem. C 123 (17) (2019) 11151–11161.
[15] K.W. Krämer, D. Biner, G. Frei, H.U. Güdel, M.P. Hehlen, S.R. Lüthi, Hexagonal sodium yttrium fluoride based green and blue emitting upconversion phosphors, Chem. Mater. 16 (7) (2004) 1244–1251.
[16] J.-C.G. Bünzli, S.V. Eliseeva, Basics of lanthanide photophysics, Lanthanide Luminescence (2010) 1–45.
[17] Y. Kitagawa, P.P.F. da Rosa, Y. Hasegawa, Charge-transfer excited states of π- and 4f-orbitals for development of luminescent Eu (iii) complexes, Dalton Trans. (2021).
[18] H. Xu, S. Han, R. Deng, Q. Su, Y. Wei, Y. Tang, X. Qin, X. Liu, Anomalous upconversion amplification induced by surface reconstruction in lanthanide sublattices, Nat. Photonics 15 (10) (2021) 732–737.
[19] G. Kresse, J. Furthmüller, Efficiency of ab-initio total energy calculations for metals and semiconductors using a plane-wave basis set, Comput. Mater. Sci. 6 (1) (1996) 15–50.
[20] P.E. Blöchl, Projector augmented-wave method, Phys. Rev. B 50 (24) (1994) 17953.
[21] J.P. Perdew, K. Burke, M. Ernzerhof, Generalized gradient approximation made simple, Phys. Rev. Lett. 77 (18) (1996) 3865.
[22] J.P. Perdew, K. Burke, M. Ernzerhof, Generalized gradient approximation made simple, Phys. Rev. Lett. 78 (7) (1997) 1396.
[23] J. Heyd, G.E. Scuseria, M. Ernzerhof, Hybrid functionals based on a screened Coulomb potential, J. Chem. Phys. 118 (18) (2003) 8207–8215.
[24] J. Heyd, G.E. Scuseria, M. Ernzerhof, Hybrid functionals based on a screened Coulomb potential, J. Chem. Phys. 124 (21) (2006) 219906.
[25] C.G. Van de Walle, J. Neugebauer, First-principles calculations for defects and impurities: Applications to III-nitrides, J. Appl. Phys. 95 (8) (2004) 3851–3879.